# A complex variable method for the floating-body boundary-value problem

Martin Greenhow

*Department of Mathematics and Statistics, Brunel University, Uxbridge, United Kingdom*

*Abstract*

Greenhow, M., A complex variable method for the floating-body boundary-value problem, Journal of Computational and Applied Mathematics 46 (1993) 115–128.

This paper reviews the use of a method using Cauchy's theorem, which has recently formed the basis of very successful numerical schemes for considering the nonlinear water-wave problem, both with and without floating or submerged bodies. Outstanding problems, concerning the intersection point problem (where two boundary conditions are to be applied) and the treatment of radiation conditions, are outlined. Notwithstanding these difficulties, useful results for transient problems may be obtained; examples presented include new results for water exit of a wedge and horizontal motion of a submerged cylinder.

*Keywords:* Floating body; free-surface flows; water exit; horizontal motion of submerged cylinder.

## 1. Introduction

The development of complex variable methods is intimately connected with that of inviscid fluid dynamics, normally used in the study of water waves, and their interaction with floating bodies. Under the usual assumptions of irrotationality, we can define a velocity potential $\Phi$ with the fluid velocity vector $v = (u, v, w) = \nabla\Phi$. If the fluid is also incompressible, this implies the field equation for $\Phi$ is Laplace's equation $\nabla^2\Phi = 0$. An alternative viewpoint, valid for two-dimensional flow $v = (u, v)$ in the $xy$-plane, is to introduce the stream function $\Psi$ with the property that

$$u = \frac{\partial\Phi}{\partial x} = \frac{\partial\Psi}{\partial y}, \qquad v = \frac{\partial\Phi}{\partial y} = -\frac{\partial\Psi}{\partial x}. \tag{1}$$

These are the Cauchy–Riemann equations for the real and imaginary parts of the complex potential $\beta(z, t) = \Phi(x, y, t) + \mathrm{i}\Psi(x, y, t)$. Here $z = x + \mathrm{i}y$ and $t$ is time. Consequently, any

*Correspondence to*: Dr. M. Greenhow, Department of Mathematics and Statistics, Brunel University, Uxbridge, Middlesex, UB8 3PH United Kingdom. e-mail: martin.greenhow@brunel.ac.uk.

$$\frac{\partial \eta}{\partial t} + \frac{\partial \Phi}{\partial x}\frac{\partial \eta}{\partial x} = \frac{\partial \Phi}{\partial z}$$

$$\frac{\partial \Phi}{\partial t} + \frac{1}{2}(\nabla\Phi)^2 + g\eta = 0$$

$z = 0$

$z = \eta(x, t)$

radiated

← waves

radiated

$\nabla^2\Phi = 0$

$\frac{\partial \Phi}{\partial n} = v_n$

waves →

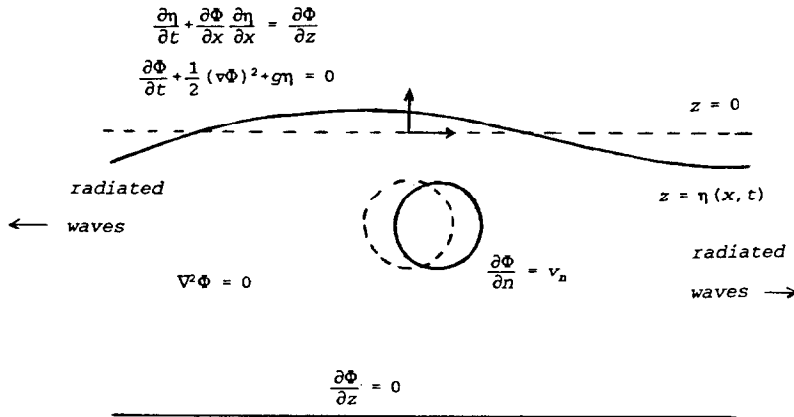$$\frac{\partial \Phi}{\partial z} = 0$$

Fig. 1. The nonlinear boundary-value problem.

complex potential may be thought of as a flow (although solid boundaries may need to be introduced, for example, along branch cuts) and, more pertinently, any fluid flow may be described by an analytic function.

Two consequences immediately follow from this formulation. Firstly, many of the elementary functions correspond to useful flows, examples being $\log(z)$, which is a source, sink or vortex (depending on its coefficient), and $\exp(-ikz)$ which gives linearised water waves of wavenumber $k$ (oscillation in $x$ and exponential decay in $-y$, i.e., depth below the free surface), see, e.g., [30,36]. Secondly, any flow may be conformally mapped to another fluid flow. This technique is particularly useful for finding the added mass of certain bodies moving in unbounded fluid, if the flow around them can be mapped to uniform flow. The added mass can then be deduced from the large $z$ behaviour, being related to the dipole moment (coefficient of the $1/z$ term), so it is not necessary to solve for the more complicated flow local to the body, see [33,41] for examples of simple body shapes. More complicated shapes may be treated by discretisation and the Schwarz–Christoffel mapping.

These analytical techniques are, however, only successful for rather simple flow domains satisfying simple conditions (usually zero normal flow) on the domain boundary. The water wave problem, and the related problems of floating or submerged bodies outlined in Sections 2 and 3 respectively, are both interesting and hard because of the complicated nonlinear free-surface boundary conditions, see Fig. 1. Although some progress had been made for rather idealised problems, such as steady waves over a wavy seabed [22] or over a flat bottom [38], and the zero-gravity entry of a wedge [21], the numerical solution of problems including both time dependence and gravity were not practical until the work of Nichols and Hirt [34], who discretised the entire fluid domain. Although some success was achieved for the early stages of water entry of a cylinder, the method was computationally expensive and not suitable for more general problems.

A breakthrough occurred when Longuet-Higgins and Cokelet [26] formulated the problem as a boundary-value problem, requiring solution and evolution only on the free-surface boundary. Since their interest was in periodic, but unsteady, flow of water waves as they break, they closed the contour of integration by a conformal map ($\zeta = \exp(-iz)$) which wraps the contour around joining the two vertical parts of the contour shown in Fig. 2; this then ensures periodicity, with
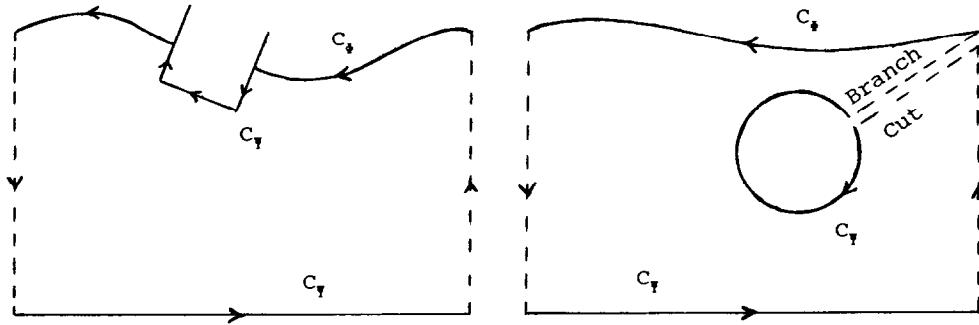
Fig. 2. Contours of integration. $C_\Phi$ and $C_\Psi$ denote parts of $C$ on which either $\Phi$ or $\Psi$ is known. Radiation or periodic conditions are applied on the vertical boundaries.

large depths being mapped to the origin. A Green's function technique was then applied in this mapped plane, resulting in a Fredholm integral equation of the first kind for the unknown normal fluid velocity at the free surface. The solution, when evolved in time according to the (transformed) dynamic free-surface boundary conditions, see Section 2, developed a saw-tooth instability which required smoothing. Nevertheless, the method, when mapped back to the physical plane, gives spectacular results for the development of wave overturning, and the high velocities and accelerations in the overturning and jet regions are of significant engineering interest. Longuet-Higgins and Cokelet [27] also applied their method to the instability growth rates of steep waves, obtaining very impressive agreement with earlier analytical theories.

Further developments of the Longuet-Higgins and Cokelet method include that of New et al. [32] who considered waves in finite-depth water (the mapped region then becomes an annulus with the Green's function satisfying the bottom boundary condition a priori). Despite the somewhat artificial nature of the initial conditions used in all the above calculations (i.e., a sinusoidal wave of large amplitude, which may be further perturbed by applying a surface pressure or modifying the water depth), the final stages of overturning are convincing. This leads to the idea that wave breaking may be, in some sense, self-similar, and that the crest region is largely uncoupled from the rest of the wave during overturning. Thus Longuet-Higgins [24,25], New [31] and Greenhow [12] have proposed local models for the loop and jet regions.

Other authors have used finite-amplitude, steady wave theories, such as that of [38], as being more realistic initial conditions. Tanaka et al. [40], Cooker et al. [8] and Cooker and Peregrine [7] took solitons as initial conditions for waves in shallow water. They considered instabilities, motion over semicircular obstructions on the seabed, and solitons in head-on collision. This last situation represents a single soliton impacting on a vertical seawall, and was shown, in some cases, to develop extremely high pressures, and accelerations of the order of hundreds, or even thousands, of $g$ in a very small impact region. Clearly very small time and space discretisations need to be made for accurate calculations.

All of the above theories become invalid when the breaking wave jet falls onto the front surface of the wave, and the numerical schemes quickly break down. This is, of course, to be expected since the flow region is no longer simply connected, and within the loop region, the analytic continuation of $\beta(z, t)$ fails to remain analytic. Thus the jet must have moved onto a different Riemann sheet, and its space derivatives will no longer match those of the front face of the wave: this results in splashing at the jet impact region, and the loop flow soon develops

into a large vortex which propagates into the fluid. The problem of continuing the calculations after jet touch-down is therefore a formidable challenge. A possible way forward is to keep track of the two layers of fluid from the wave front and jet respectively, and to apply a boundary condition across the interface of a jump in potential which conserves the Kelvin impulse. This method has been successfully to study the collapse beyond jet re-entry of axisymmetric bubbles, see [3].

Although conformal mappings are used in the above numerical schemes, the problem is not formulated directly in terms of the complex velocity potential $\beta(z, t)$. One possibility is to construct $\beta$ from singularities exterior to the fluid region, choosing their coefficients in such a way as to minimise the errors when satisfying the free-surface conditions, see [29]. Another is to construct $\beta$ from a vortex sheet placed at the free surface; the (unknown) strength distribution and its evolution are determined by the free-surface conditions, see [2]. Since the governing Fredholm equations are of the second kind with globally convergent Neumann series, the resulting matrix equations may be solved iteratively — a significant advantage over direct Gaussian elimination methods.

Since $\beta$ is analytic, Cauchy's theorem holds:

$$\oint_C \frac{\beta(z, t)}{z - z_0} \, dz = 0, \tag{2}$$

for any contour $C$ drawn within the fluid or along its boundary, and with $z_0$ outside $C$. Evidently, any other analytic function will satisfy this equation; to evolve the solution, we will need (2) with $\partial\beta/\partial t$ in place of $\beta$, see Section 2. Another possibility includes the velocity potential gradient as a function of $w = u + iv$, which results in an integral equation for the (unknown) normal derivative of $\Phi$, see [9]. An interesting feature of that paper is that the higher time derivatives of the analytic function may be easily calculated since the kernel of the integral equation is the same. Knowing these enables much larger time steps to be taken for any given accuracy.

Section 2 outlines the method of Vinje and Brevig [45]. The major difference is that Vinje and Brevig do not build in periodicity of the flow into their method (by mapping the contour $C$, or otherwise), but rather solve (2) directly in the physical plane. Thus, although periodic waves and flows may be considered, their method has the advantage that other conditions may be applied at the vertical boundaries, and more importantly, floating or submerged bodies may be introduced. In these cases periodicity at the vertical boundaries is not appropriate and one needs to apply a radiation condition at these boundaries to account for the outgoing diffracted waves, and any waves radiated by a moving body. This problem has not been satisfactorily resolved, see [5,46]. These authors attempt to match the interior nonlinear region with a linear outer region satisfying the Orlanski condition [35]

$$\frac{\partial\Phi}{\partial t} = -C\frac{\partial\Phi}{\partial x}, \tag{3}$$

where $C$ is calculated from the rate of change of $\Phi$ in the interior region. (Using $C$ from the phase speed of linearised waves the Somerfeldt condition was also tried.) The results, which always gave some reflection, were disappointing. A further problem was that the nonlinear (finite-amplitude) waves in the interior region do not decay in amplitude as they propagate
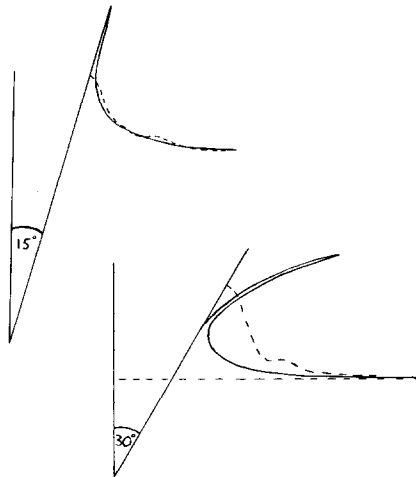
Fig. 3. Wedge entry at high speed. Note that the spray may separate from the wedge side. The analytic results of Appendix 1 are shown dotted.

outwards, and were therefore difficult to match to the outer domain which has boundary conditions applied at the undisturbed free-surface level. This is in contrast to the three-dimensional situation where wave amplitude decays like $1/\sqrt{R}$, and where the inner and outer regions may be matched successfully, see [23].

More pragmatic approaches appear to work well in some situations. For example, for the problem of water entry or water exit into otherwise calm water, it is possible to place the vertical boundaries sufficiently far away, so that no significant disturbance reaches them during the transient phase of interest, see Fig. 3. Another successful technique was used for waves moving over a submerged cylinder [6]. For this case the transmitted wave propagated into an "energy sponge" region where its amplitude was artificially reduced to zero at the end wall. This apparently gave insignificant reflection back into the physical region of interest around the cylinder. A similar technique has been applied in [1].

## 2. The method of Vinje and Brevig

The contour integral of Cauchy's theorem above may be split into two parts: $C_\Phi$ where $\Phi$ is known and $C_\Psi$ where $\Psi$ is known, see Fig. 2; these quantities are either specified initially or known from the evolution equations below. Thus $\Phi$ and its time derivative are known on the free surface ($\partial\Phi/\partial t$ is given from the Bernoulli equation), while $\Psi$ and its time derivative are known on the bottom (both are zero here) and, if present, on a body surface ($\Psi$ and $\partial\Psi/\partial t$ are here specified by the body geometry and its velocity). Taking $z_0$ ($=x_0 + iy_0$) on the contour $C$, and using either the real or imaginary parts of (2) gives integral equations of the second kind:

$$\pi\Psi(x_0, y_0, t) + \mathrm{Re}\left[\int_C \frac{\Phi + i\Psi}{z - z_0}\,\mathrm{d}z\right] = 0, \tag{4}$$

for $z_0$ on $C_\Phi$, and

$$\pi\Phi(x_0, y_0, t) + \text{Re}\left[i\int\frac{\Phi + i\Psi}{z - z_0}\,dz\right] = 0, \tag{5}$$

for $z_0$ on $C_\Psi$. Similar equations hold for the time derivative of $\beta$. We have further assumed that $C$ is smooth; at corners, either due to the presence of a solid body or due to discretisation of $C$, we use the angle subtended by the collocation points $\epsilon_N$ in place of $\pi$ in these equations. On the vertical boundaries in Fig. 2, we apply either periodicity, or an appropiate fixed wall or wavemaker condition, making it part of $C_\Psi$.

To step forward in time we use the boundary conditions for the two-dimensional free-surface problem as given in Fig. 1 (for a derivation see, e.g., [36]). Following [26], we write the free-surface conditions following a free-surface particle (a Lagrangian description of the flow) as

$$\frac{\text{D}z}{\text{D}t} = u + iv = w^* = \frac{\partial\beta}{\partial z}, \qquad \frac{\text{D}\Phi}{\text{D}t} = ww^* - gy - \frac{P_s}{\rho}, \tag{6}$$

where $g$ is the gravity, $\rho$ the density, and the material derivative is given by

$$\frac{\text{D}(\cdot)}{\text{D}t} = \frac{\partial(\cdot)}{\partial t} + \nabla\Phi\,\nabla(\cdot). \tag{7}$$

These equations are used to evolve the position and value of $\Phi$ of the free-surface particles to the next time step. Specifically a single-step Runge–Kutta method is used to calculate the first three steps, after which we may use a fourth-order Hamming predictor/corrector method. A numerical derivative of $\beta$ is calculated. The forces on the body (if present) are calculated by integrating the hydrodynamic pressure, given by Bernoulli's equation, over its surface; this gives its acceleration and hence its new position and velocity. For further details see [15,44].

As mentioned above, the collocation method is applied to (4) and (5). Assuming a linear variation between the collocation points, Vinje and Brevig perform the integrations analytically. This results in an $N \times N$ matrix equation $AX = B$ for the unknown part $X$ of $\beta$ at each of the $N$ collocation points. The elements of the $N \times N$ matrix $A$ consist of logarithmic terms, requiring typically 40% of the calculation time for their evaluation. However, the matrix is also used at each time step for the calculation of the unknown part of $\partial\beta/\partial t$, and could also be used for the calculation of higher derivatives of $\beta$, as in the method of [9].

When no body is present, it may be advantageous to use an iterated scheme to solve the matrix equation, since we have an excellent initial guess given by the solution at the previous time step, see [2,23]. Against this, we have already noted that the calculation time of $A$ is dominant, and iteration becomes awkward if we wish to apply regridding of the collocation points, see [10]. That paper illustrates the power of this method: a comparison of experimental and numerical wave tanks, both given identical wavemaker motions, is made for the wave profile at various positions along the tanks. With 550 unknowns and about 4000 time steps, the results agree very well, even to the resolution of wave breaking. The entire simulation took about 30 hours on a CRAY 1 supercomputer.

In the case of ship motion, and particularly for the water-entry and -exit cases presented here, we note that the number of collocation points $N$ continually changes as the body submerges or emerges; here we use direct Gaussian elimination. A further problem for

surface-piercing bodies occurs at the intersections of the free and body surfaces. Except in special cases, the complex velocity potential $\beta$ or its time derivatives are known to be singular here, see, e.g., [39,43]. The introduction of viscosity may, in principle, be needed. In the present formulation, we have both $\Phi$ and $\Psi$ specified at these points. Although no theoretical justification exists, we remove the two intersection points from the calculations and solve an $(N-2) \times (N-2)$ system of equations. Then, treating the intersection points as ordinary free-surface points for the purposes of time stepping appears to give acceptable results, see [23] for the wavemaker problem and [13,14] for wedge and cylinder entry. These cases may be compared with theoretical results. For the impulsively-moving wavemaker case, the numerical results lie very close to the theoretical free-surface profile (which is logarithmic, see [37]), except near to the intersection point. For high speed wedge entry, the self-similarity of the flow has the consequence that the arc length along the free surface between any two free-surface particles is maintained, see [11]. The results of [13] satisfy this stringent check, and other checks such as mass conservation, accurately only for slender wedges. When the deadrise angle (the angle between the body and free surface) becomes smaller than 45°, the calculations become unreliable and quickly break down. Resolution problems arise because of the spray jets of fluid which move up the side of the wedge at great speed, see Fig. 3. Furthermore, the initial condition for this problem is itself singular: thus resolving the jets more accurately does not remove the problem, but rather makes it worse. Zhao and Faltinsen [49] point out that the pressure in these jets is almost atmospheric, and claim success for deadrise angles as small as 15° by simply truncating the jets with an artificial boundary on which the pressure is atmospheric. A better procedure may be to match to an analytic model of the outer (jet) region as in the analytical work of [20,47].

A similar problem arises for the case of wedge exit; we present new results in Fig. 4. Although no jets occur, the intersection point particles still move very quickly for small deadrise angles. Some free-surface profiles are shown in Fig. 4, together with a comparison with the transient linear wavemaker theory of [28], which is expected to be valid for slender wedges
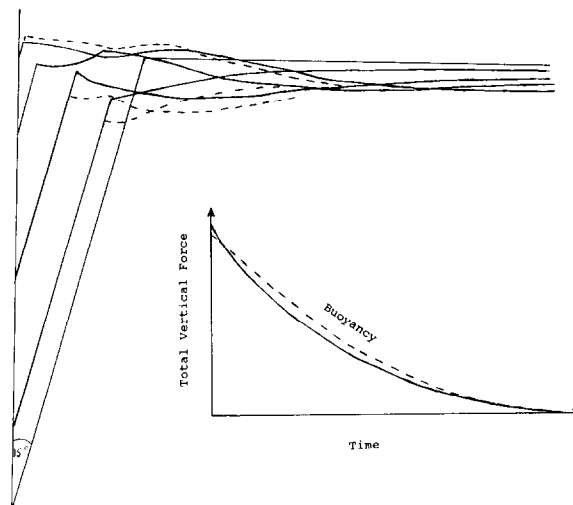


Fig. 4. Wedge exit from initially calm water. On the left part the analytic results of Appendix 1 are shown dotted, while on the right part the dotted line shows the contribution of buoyancy according to linear theory.

(deadrise angles approaching 90°). Analytical results for the free-surface profile for water entry and water exit are given in Appendix 1. For smaller deadrise angles, no simple analytical theory is yet available. (Unlike the high-speed water-entry case, we must here include both gravity and the length scale of the initial submergence depth; thus the problem is Froude number $F_r$ dependent.)

For submerged bodies, we do not, of course, have the above intersection point problems. However, a difficulty does arise with the integration around the contour, which now involves a branch cut. We account for this when integrating around inner and outer contours in Fig. 2 (right part). Furthermore, for a fixed body, we do not know the constant value of $\Psi$ on its surface. However, referring to (5), we see that integrating around the cylinder gives

$$\oint_{\text{cyl}} \frac{i\Psi}{z - z_0} dz = i\Psi \oint_{\text{cyl}} \frac{dz}{z - z_0} = 0,$$ (8)

when $z_0$ is outside the cylinder, and

$$\text{Re}\left[ i \oint_{\text{cyl}} \frac{i\Psi}{z - z_0} dz \right] = \text{Re}[\pi i \Psi] = 0,$$ (9)

when $z_0$ is on the cylinder. Thus the unknown constant value of $\Psi$ is immaterial, but may be calculated around the cylinder from (4) as a check. For the moving cylinders considered here, we do know the variation of $\Psi$ around the cylinder from the body boundary condition to within this unknown constant value, see [4] for details. More general initial conditions, where the circulation around the cylinder and hence the value of $\Psi$ are specified, can also be considered, see [42].

The other new results presented here concern the impulsive horizontal motion of a submerged circular cylinder. The corresponding steady motion problem has been extensively studied by Havelock [17], using the linearised free-surface condition. When the cylinder is sufficiently deeply submerged and moving sufficiently slowly, his results agree well with the numerical schemes of [1,16]. The present results concentrate on transient motion of the cylinder very near the free surface. Appendix 2 presents and extends Havelock's [18] theory for this situation. We see in Fig. 5, taken from [19], that the assumptions of linearity, as well as the approximate nature of the satisfaction of the body boundary condition, preclude the use of the analytical results in Appendix 2, unless the body is very deeply submerged. However, the numerical scheme is capable of dealing with high speeds at quite small submergences.

## 3. Conclusions

Over the past fifteen years, some fast and reliable programs have been developed for the nonlinear water wave problem. We can now calculate the modulation of a wavetrain, interactions between waves or solitons, and overturning of a wave crest; such work has further stimulated analytical work. For two dimensions, the main outstanding problems appear to be

    (i) the successful implementation of radiation conditions, so that the computational domain may be kept small;

    (ii) a satisfactory way of treating the intersection points for surface-piercing bodies, especially when the deadrise angles are small; and
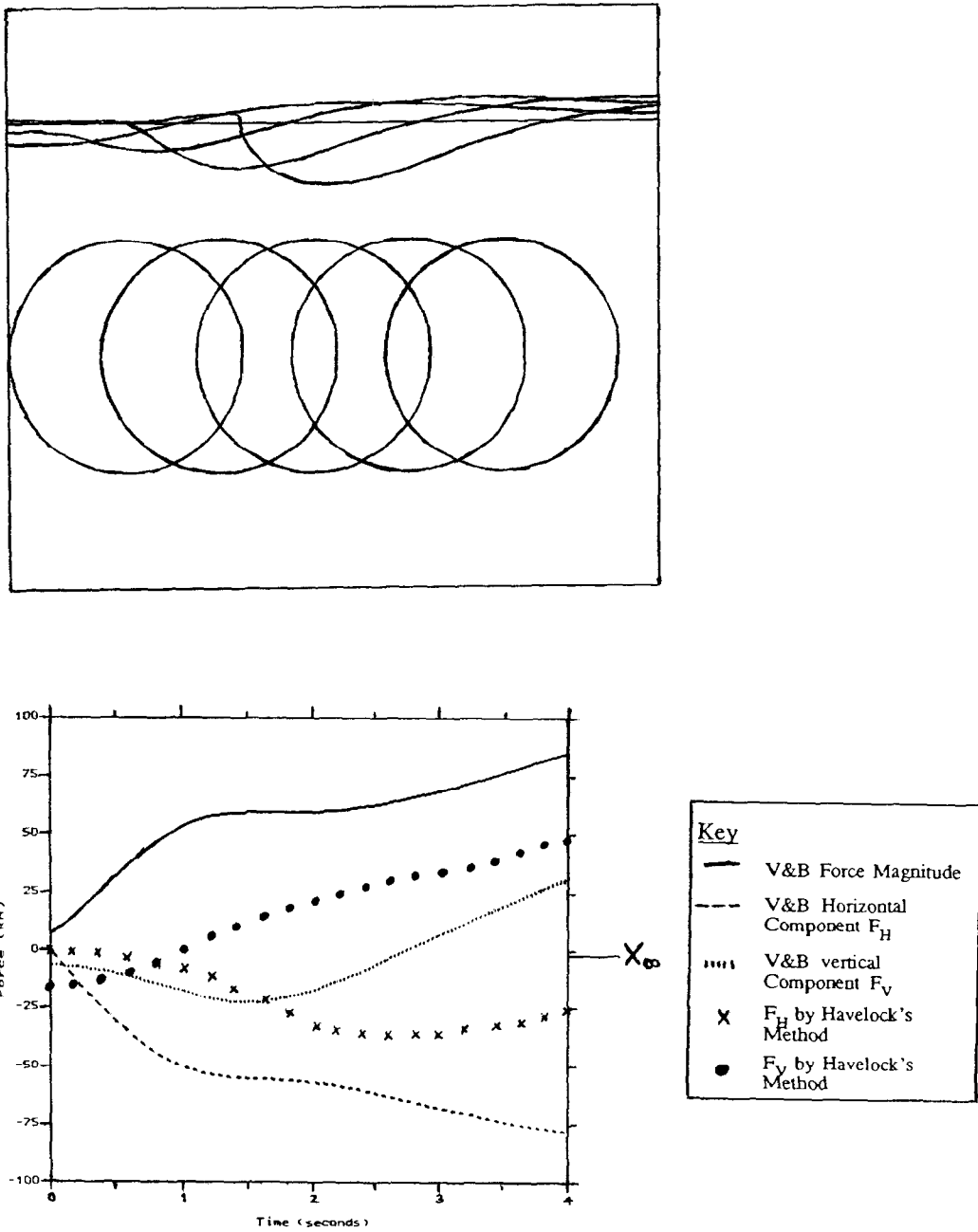
Fig. 5. Impulsive motion of a horizontal submerged cylinder. The analytic results for the forces are shown dotted. This figure is taken from [19].

(iii) a theoretical framework for treating waves after breaking, and its numerical implementation.

When bodies are introduced, or waves are generated by a wavemaker, the most successful approach to date appears to be that of [44,45], described in Section 2. Although the method

may be applied to the large computational domain of a "numerical wave tank", as in [10], many interesting calculations may be made at modest cost by considering transient problems where the initial conditions may be given exactly. Examples of water entry and water exit, and the motion of submerged bodies have been presented; the results are compared with those from linear theories given in the appendices.

## Appendix 1

For comparison with the numerical results calculated by the Vinje and Brevig method we here extend the transient wavemaker theory of Mackie [28]. Mackie considers the entry of a solid wedge of half-angle $\epsilon$; if the wedge is slender ($\epsilon$ is small), it is appropriate to use the linearised free-surface condition, see, e.g., [36],

$$\frac{\partial^2 \Phi}{\partial t^2} - g\frac{\partial \Phi}{\partial y} = 0, \quad \text{applied on } y = 0. \tag{10}$$

The free-surface elevation is given by

$$\eta(x, t) = \frac{1}{g}\left(\frac{\partial \Phi}{\partial t}\right). \tag{11}$$

The body boundary condition is not applied on the wedge surface, but rather on an "equivalent wavemaker" at $x = 0$, satisfying

$$\frac{\partial \Phi}{\partial x} = u(y, t), \quad \text{on } x = 0. \tag{12}$$

Here $u(y, t)$ is chosen to simulate the motion of the wedge, i.e.,

$$u(y, t) = \begin{cases} u\epsilon, & \text{for } 0 \leqslant y < ut, \\ 0, & \text{for } y > ut, \end{cases} \tag{13}$$

for wedge entry at constant velocity $u$, and

$$u(y, t) = \begin{cases} u\epsilon, & \text{for } 0 \leqslant y \leqslant d + ut, \\ 0, & \text{otherwise}, \end{cases} \tag{14}$$

for wedge exit at constant velocity $u$, with the vertex initially at depth $d$.

Mackie solves the general problem by Fourier and Laplace transforms; the Fourier transform of the free-surface elevation

$$H(\lambda, t) = \int_0^\infty \eta(x, t) \cos(\lambda x)\, \mathrm{d}\lambda \tag{15}$$

is given by

$$H(\lambda, t) = -\int_0^\infty U(\lambda, t) \cos\left[\sqrt{\lambda g}\,(t - \tau)\right] \mathrm{d}\tau, \tag{16}$$

where $U(\lambda, t)$ is the Fourier transform of $u(x, t)$. This expression may be interpreted as a

convolution over the previous history of wavemaker motion $U(\lambda, \tau)$ from $\tau = 0$ to the present time $t$. Substituting the Fourier transforms $U(\lambda, t)$ for the entry and exit problems gives

$$H(\lambda, t) = -\epsilon u^2 \left[ \frac{e^{-\lambda u t} - \cos\left(\sqrt{\lambda g}\, t\right) + u\sqrt{\lambda g^{-1}}\,\sin\left(\sqrt{\lambda g}\, t\right)}{\lambda^2 u^2 + \lambda g} \right] \tag{17}$$

and

$$H(\lambda, t) = \frac{\epsilon u\, e^{-\lambda d}}{\lambda} \left[ \frac{\lambda u\left[\cos\left(\sqrt{\lambda g}\, t\right) - e^{-\lambda u t}\right]}{\lambda^2 u^2 + \lambda g} + \sin\left(\sqrt{\lambda g}\, t\right)\sqrt{\lambda g} \left[ \frac{1}{\lambda^2 u^2 + \lambda g} - \frac{e^{\lambda d}}{\lambda g} \right] \right], \tag{18}$$

respectively. We then take the inverse Fourier transform

$$\eta(x, t) = \frac{2}{\pi} \int_0^\infty H(\lambda, t) \cos(\lambda x)\, d\lambda \tag{19}$$

to give the profiles shown dotted in Figs. 3 and 4. For slender wedges there is quite good agreement with the numerical results. In these figures, we have started drawing the free-surface profiles not at $x = 0$, but at the wedge surface. Although this is sensible, we note that the necessity of making such a choice arises from the inadequacy of the above theory to account properly for the actual wedge profile. This inadequacy is likely to result in serious error for wedges which are not slender. Indeed, we see immediately that, according to this (linear) theory, the above profiles are linear in $\epsilon$ (the half-angle of the wedge). Another source of disagreement may be that for nonslender wedges the free-surface deformations are so steep that the linearised boundary condition (10) is likely to give serious errors. Nevertheless, when applied to appropiate cases, the above analytic results are capable of providing a simple explanation of the numerical results, and, since gravity is included, the analytic solutions evolve to give realistic wavetrains (not shown in Figs. 3 and 4).

## Appendix 2

We here present and extend the dipole theory of Havelock [18] for the impulsive horizontal motion of a horizontal cylinder with axis at depth $d$. In unbounded fluid (i.e., no free surface present) the flow around a cylinder of radius $r$, moving horizontally with velocity $u$, is given by a dipole $\beta(z, t) = ur^2/z$. The effect of free-surface proximity is to introduce an image of this dipole plus a memory term representing radiated waves:

$$\beta(z, t) = \frac{ur^2}{z} - \frac{ur^2}{z - 2id}$$

$$+ ur^2\sqrt{g} \int_0^t d\tau \int_0^\infty \left[ e^{ik(u - (g/k)^{1/2})(t - \tau)} - e^{-ik(u - (g/k)^{1/2})(t - \tau)} \right] e^{-ik - 2kd}\sqrt{k}\, dk. \tag{20}$$

In this case the force $Z = X + iY$ may be obtained from the Blasius theorem (the time-dependent terms are nonsingular and therefore do not contribute to the contour integral). Thus

$$Z = -\tfrac{1}{2}\rho i \oint \left(\frac{d\beta}{dz}\right)^2 dz. \tag{21}$$

This gives Havelock's result for the horizontal force, or resistance $X$:

$$X = 4\pi g\rho r^4 \kappa_0^2 \int_0^\infty \left[\frac{\sin(\alpha\gamma(\gamma - 1))}{\gamma - 1} - \frac{\sin(\alpha\gamma(\gamma + 1))}{\gamma + 1}\right]\gamma^5 e^{-\delta\gamma^2}\, d\gamma, \tag{22}$$

where

$$\kappa_0 = \frac{g}{u^2}, \qquad \alpha = \kappa_0 ut, \qquad \delta = 2\kappa_0 d. \tag{23}$$

The vertical force $Y$ is given by

$$Y = \frac{-4\pi\rho r^4 g^3}{u^4}\left[\frac{u^6}{8g^3 d^3} + \int_0^\infty \left[\frac{1 - \cos(\alpha\gamma(\gamma - 1))}{\gamma - 1}\right.\right.$$
$$\left.\left. - \frac{1 - \cos(\alpha\gamma(\gamma + 1))}{\gamma + 1}\right]\gamma^5 e^{-\delta\gamma^2}\, d\gamma\right]. \tag{24}$$

Following [18], we use the method of stationary phase to give the large time asymptotics of these expressions. Thus

$$X \to -4\pi g\rho\kappa_0^2 r^4\left[\pi e^{-\delta} - \frac{1}{16}\sqrt{\frac{\pi}{\kappa_0 ut}}\; e^{-\delta/4}\, \sin\left(\tfrac{1}{4}(\pi - \kappa_0 ut)\right)\right] \tag{25}$$

and

$$Y \to \frac{-\pi\rho r^4 g}{d^4}\left[\frac{1}{\delta} + 1 + \delta - \delta^2 e^{-\delta}Ei(\delta) + \tfrac{1}{16}\delta^2 e^{-\delta/4}\frac{\pi}{\sqrt{\kappa_0 ut}}\cos\left(\tfrac{1}{4}(\pi - \kappa_0 ut)\right)\right]. \tag{26}$$

The first terms, which arise from a singularity on the contour of integration, represent the steady-state forces and correspond to the forces calculated from the steady (nonimpulsive) motion problem, see [48], after correcting a sign in their expressions. The last terms are oscillatory. The numerical calculations are qualitatively similar for the very deeply submerged cylinder case, although for initial stages of the motion the numerical and analytic results disagree significantly. For cylinders near the surface, as shown in Fig. 5, the theories disagree significantly, as we might expect in such a nonlinear situation, and a comparison of the large time results is not possible because the numerical results produce a large wave which breaks, terminating the calculations.

# References

[1] G.R. Baker, D.I. Merion and S.A. Orszag, Application of a generalised vortex method to nonlinear free surface flows, in: J.H. McCarthy, Ed., *Proc. Third Conf. Ship Hydrodynamics*, Paris (Office of Naval Research, 1981) III-3-1–III-3-13.

[2] G.R. Baker, D.I. Merion and S.A. Orszag, Generalised vortex methods for free-surface flow problems, *J. Fluid Mech.* **123** (1982) 477–501.

[3] J.P. Best, The dynamics of underwater explosions, Ph.D. Thesis, Univ. Wollongong, Australia, 1991.

[4] P. Brevig, M. Greenhow and T. Vinje, Extreme wave forces on submerged cylinders in: *Proc. 2nd BHRA Internat. Symp. on Wave and Tidal Energy*, Cambridge (British Hydraulics Research Assoc., 1981) 143–166.

[5] T. Christiansen, An investigation of non-linear wave motion, Report No. 2.9, NTNF Research Program, A.S. Veritec, Oslo, 1986.

[6] R. Cointe, Waves travelling over a submerged cylinder: nonlinear vs. second-order theory, in: J. Grue, Ed., *Proc. 4th Internat. Workshop on Water Waves and Floating Bodies*, Østese, Norway, 1989, 39–43.

[7] M. Cooker and D.H. Peregrine, Computation of violent motion due to waves breaking against a wall, *Proc. Coastal Engrg.* **1** (1990) 164–176.

[8] M. Cooker, D.H. Peregrine, C. Vidal and J.W. Dold, The interaction between a solitary wave and a submerged semicircular cylinder, *J. Fluid Mech.* **215** (1990) 1–22.

[9] J.W. Dold and D.H. Peregrine, Steep unsteady water waves: an efficient computational scheme, Report No. AM-84-04, School Math., Univ. Bristol, 1984.

[10] D.G. Dommermuth, D.K. Yue, W.-M. Lin, R.J. Rapp, E.S. Chan and W.K. Melville, Deep-water plunging breakers: a comparison between potential theory and experiments, *J. Fluid Mech.* **189** (1988) 423–442.

[11] P.R. Garabedian, Oblique water entry of a wedge, *Comm. Pure Appl. Math.* **6** (1953) 157–165.

[12] M. Greenhow, Free-surface flows related to breaking waves, *J. Fluid Mech.* **134** (1983) 259–275.

[13] M. Greenhow, Wedge entry into initially calm water, *Appl. Ocean Res.* **9** (4) (1987) 214–223.

[14] M. Greenhow, Water-entry and -exit of a horizontal circular cylinder, *Appl. Ocean Res.* **10** (4) (1988) 191–198.

[15] M. Greenhow, T. Vinje, P. Brevig and J. Taylor, A theoretical and experimental study of the capsize of Salter's duck in extreme waves, *J. Fluid Mech.* **118** (1982) 221–239.

[16] H.J. Haussling and R.M. Coleman, Nonlinear water waves generated by an accelerating circular cylinder, *J. Fluid Mech.* **92** (1979) 767–781.

[17] T.H. Havelock, The forces on a circular cylinder submerged in a uniform stream, *Proc. Roy. Soc. London Ser. A* **157** (1936) 526–534.

[18] T.H. Havelock, The wave resistance of a cylinder started from rest, *Quart. J. Mech. Appl. Math.* **22** (2) (1949) 401–414.

[19] T. Hepworth, An investigation of the motion of a submerged cylinder moving below a free surface with constant velocity, 4th year project report, Dept. Math. Statist., Brunel Univ., 1991.

[20] S.D. Howison, J.R. Ockendon and S.K. Wilson, Incompressible water-entry problems at small deadrise angles, *J. Fluid Mech.* **222** (1991) 215–230.

[21] O.F. Hughes, Solution of the wedge entry problem by numerical conformal mapping, *J. Fluid Mech.* **56** (1) (1972) 173–192.

[22] F. John, Two-dimensional flows with a free boundary, *Comm. Pure Appl. Math.* **6** (1953) 497–503.

[23] W.-M. Lin, J.N. Newman and D.K. Yue, Nonlinear forced motions of floating bodies, in: W.C. Webster, Ed., *15th Symp. Naval Hydrodynamics*, Hamburg (National Academy Press, Washington, DC, 1984) 33–49.

[24] M.S. Longuet-Higgins, Parametric solutions for breaking waves, *J. Fluid Mech.* **121** (1982) 403–424.

[25] M.S. Longuet-Higgins, Rotating hyperbolic flow: particle trajectories and parametric representation, *Quart. J. Mech. Appl. Math.* **36** (1983) 247–270.

[26] M.S. Longuet-Higgins and E.D. Cokelet, The deformation of steep surface waves on water. I. A numerical method of computation, *Proc. Roy. Soc. London Ser. A.* **350** (1976) 1–26.

[27] M.S. Longuet-Higgins and E.D. Cokelet, The deformation of steep surface waves on water. II. Growth of normal mode instabilities, *Proc. Roy. Soc. London Ser. A* **364** (1978) 1–28.

[28] A.G. Mackie, Gravity effects in the water entry problem, *J. Austral. Math. Soc.* **5** (1965) 427–433.

[29] P. McIver and D.H. Peregrine, The computation of unsteady and steady free-surface motions using a small number of singularities in the exterior flow field, Report No. AM-81-13, School Math., Univ. Bristol, 1981.

[30] L.M. Milne-Thompson, *Theoretical Hydrodynamics* (Macmillan, New York, 5th ed., 1986).

[31] A.L. New, A class of elliptical free-surface flows, *J. Fluid Mech.* **130** (1983) 219–239.

[32] A.L. New, P. McIver and D.H. Peregrine, Computations of overturning waves, *J. Fluid Mech.* **150** (1985) 233–251.

[33] J.N. Newman, *Marine Hydrodynamics* (MIT Press, Cambridge, MA, 1977).

[34] B.D. Nichols and C.W. Hirt, Nonlinear hydrodynamic forces on floating bodies, in: J.H. McCarthy, Ed., *2nd Internat. Conf. on Numer. Ship Hydrodynamics*, Berkeley (Office of Naval Research, 1977) 382–394.

[35] I. Orlanksi, A simple boundary condition for unbounded hyperbolic flows, *J. Comput. Phys.* **121** (1976) 251–269.

[36] A.R. Paterson, *A First Course in Fluid Dynamics* (Cambridge Univ. Press, Cambridge, 1983).

[37] D.H. Peregrine, Flow due to a vertical plate moving in a channel, Unpublished note.

[38] M.M. Rienecker and J.D. Fenton, A Fourier method for steady water waves, *J. Fluid Mech.* **104** (1981) 119–137.

[39] A.J. Roberts, Transient free-surface flows generated by a moving vertical plate, *Quart. J. Mech. Appl. Math.* **40** (1) (1987) 129–158.

[40] M. Tanaka, J.W. Dold, M. Lewy and D.H. Peregrine, Instability and breaking of a solitary wave, *J. Fluid Mech.* **185** (1987) 235–248.

[41] J.L. Taylor, Some hydrodynamic inertia coefficients, *Philos. Mag.* **9** (7) (1930) 161–183.

[42] A.F. Teles da Silva and D.H. Peregrine, Nonlinear perturbations of a free surface induced by a submerged body: a boundary integral approach, *Engrg. Analysis with Boundary Elements* **7** (1990) 214–222.

[43] T. Vinje, On the small time expansion of nonlinear free surface problems, in: J. Grue, Ed., *Proc. 4th Internat. Workshop on Water Waves and Floating Bodies*, Østese, Norway, 1989, 245–250.

[44] T. Vinje and P. Brevig, Nonlinear, two-dimensional ship motions, Ship Res. Inst. Norway R-112-81, 1981.

[45] T. Vinje and P. Brevig, Breaking waves on finite depth water; a numerical study, Ship Res. Inst. Norway R-118-81, 1981.

[46] T. Vinje, P. Brevig and M. Xie, A numerical approach to nonlinear ship motion, in: *14th Symp. Naval Hydrodynamics*, Ann Arbor (Office of Naval Research, 1982) 1–32.

[47] H. Wagner, Über Stöss- und Gleitvorgänge an der Oberflache von Flüssigkeiten, *Z. Angew. Math. Mech.* **12** (1932) 193–215; see also: *The Phenomena of Impact and Planning on Water* (N.A.C.A., 1936) Translation 1366, 1–57.

[48] J.V. Wehausen and E.V. Laitone, Surface waves, in: S. Flugge, Ed., *Handbook of Physics* **9** (Springer, Berlin, 1960) 446–778.

[49] R. Zhao and O. Faltinsen, Water entry of a two-dimensional body, in: *Proc. 6th Internat. Workshop on Water Waves and Floating Bodies*, Woods Hole, 1991.